PREPRINT of the paper published in:

Journal of Dispersion Science and Technology, 2011, V.32, Iss.8, P.1206-1212..

Thixotropy in Native Petroleum Emulsions

Igor N. Evdokimov and Aleksandr P. Losev

Department of Physics, Gubkin Russian State University of Oil and Gas, Moscow, Russia

Abstract. Native water in crude oil emulsions, stabilized by indigenous surfactants, exhibit both positive thixotropy (PT) and negative thixotropy (NT) in Couette flow. PT is associated with microscopic processes – local break-up of droplet clusters in emulsions with low and moderate volume fractions of water ϕ, or fracturing of emulsion-gels with $\phi > 0.7$. The latter process involves the coalescence of water droplets along a fracture plain, which results in vorticity banding of emulsion flow. NT reflects evolution of the macroscopic radial banding in flow of emulsions with $0.18 < \phi < 0.58$ and is dictated by the displacement of the interface between the sheared and unsheared regions.

Keywords: Emulsions, crude oils, viscosity, thixotropy.

Address correspondence to I. N. Evdokimov, Department of Physics, Gubkin Russian State University of Oil and Gas, Leninsky Prospekt, 65, Moscow B-296, GSP-1, 119991, Russia. E-mail: physexp@gubkin.ru

1 INTRODUCTION

Water-in-crude oil (W/O) emulsions continue to challenge the petroleum industry during drilling, producing, transporting and processing of crude oils.[1-5] Emulsions increase the volume and viscosity of oil which adds significantly to operating costs. Many studies have been carried out in the last decades and have led to a better understanding of these complex systems.[2] Most authors agree that emulsion properties are determined mostly by the indigenous surfactants contained in the crude, e.g. asphaltenes, resins, naphthenic acids and fine solids.[1,4] However, in spite of continuing laboratory research with specially formulated emulsions, the origin of complex rheological behavior (e.g., viscoelasticity and thixotropy[3,6]) in emulsions of native, as-recovered crude oils still remain elusive. In our previous publications,[7,8] we concluded that the rheology of native W/O emulsions of diverse geographical origin may be determined by some common morphological features. The present study is aimed at developing a better understanding of emulsion morphology and flow properties by thixotropic loop tests.[9] It is hoped that the results will provide information to aid in the production and refining operations of the petroleum industry.

2 MATERIALS AND METHODS

2.1 Materials

The virgin crude oil was collected directly from the producing well #624 at Korobkovskoye reservoir (Volgograd, Russia), had a density of 832 kg/m^3, a pour point below -18 ^{o}C, contained ca. 1 wt.% asphaltenes, 8 wt.% resins, 2 wt.% waxes, suspended fine solids not exceeding 0.4 g/L. Oil samples were stored in the dark, in air. The water in this study was a double distillate stored in air, with pH≈5.5. In emulsion studies, samples of 10 g water + oil were prepared at various weight ratios ranging from 0 to 85% (weighting accuracy 0.01 g) in standard

cylindrical glass vessels. The two phases were mixed manually by vigorously shaking and upturning a vessel (with a frequency of ~2-2.6 c^{-1}) for 10 minutes, which resulted in a visually homogeneous emulsion. A type of emulsion (W/O or O/W) was inferred by a conventional "drop test".[10] (a drop of o/w emulsion disperses in water, while a drop of w/o emulsion disperses in oil). All our emulsions, with water contents up to 85% w/w, appeared to be oil-continuous (W/O).

2.2 Experimental Procedure

Flow curves of emulsions (shear stresses σ as functions of shear rates $\dot{\gamma}$) were determined using: (1) a Brookfield DV-II+ PRO Digital Viscometer, equipped with a concentric cylinder ULA setup (spindle diameter = 25.15 mm, gap = 1.23 mm), at shear rates from 0.06 to 100 s^{-1}; (2) a Rheotest 2.1 VEB MLW Viscometer, with a concentric cylinder S-S1 setup (spindle diameter = 39.2 mm, gap = 0.4 mm), at shear rates from 0.05 to 437 s^{-1}. Temperature was controlled at 20 ^{o}C by a circulating water bath, typically to within 0.2 °C. When first loaded into the viscometer, each sample was pre-sheared by applying a lowest shear rate for 3 min. Thixotropic loop measurements were conducted in a "single trip" mode,[11] as illustrated in Figure 1. In a Brookfield viscometer, the shear rate was increased and decreased in steps. At each shear rate, the samples were equilibrated for 4-5 min, shear stress values were registered every 30 seconds. In a Rheotest viscometer, the shear rate was increased logarithmically to the highest value (typically, 400 s^{-1}) in about 1 hour and then decreased logarithmically back to zero shear conditions. At each shear rate, shear stress values were recorded after the waiting time of 1 min.

3 RESULTS AND DISCUSSION

3.1 Hysteresis of Flow Curves and Characteristic Water Cuts

The typical loop test results for emulsions with various water volume fractions (water cuts) ϕ are shown in Figure 2A. At small ϕ, the upward and downward flow curves $\sigma(\dot{\gamma})$ practically coincide and a noticeable hysteresis commences for water cut exceeding ca. 0.18, indicating a progressive breakdown/rebuilding of some structures of emulsion droplets.[9] Of immediate relevance for further discussion of hysteresis loops is evolution of the upward flow curves with increasing water cut which has been analyzed in detail in our previous publication.[7] Some of the characteristic features are summarized in Figure 2B,C.

Figure 2B shows that in spite of the obvious high degree of flocculation, all emulsions with $\phi \leq 0.64$ at low shear rates apparently behaved as Newtonian fluids with zero yield stress, while al higher water cuts the flow curves remained linear, though with a sizable yield stress (Bingham fluids). Note a special case of emulsion with $\phi = 0.82$ where a considerable drop of shear stress is due to a fracture-like loss of homogeneity under shear. Namely, there appeared clearly visible bands (streaks) of large, millimeter-sized water droplets and elongated water domains, parallel to the direction of shear, a process which may be classified as "vorticity banding".[12]

Figure 2C shows characteristic non-linear segments ("plateau") which start to appear at upward flow curves for $0.18 < \phi < 0.64$ and have been attributed to development of specific emulsion-gel structures. Comparison with various viscosity models revealed that even at $\phi < 0.18$, low-shear emulsions can not be described as dispersions of individual water droplets. The basic units of the disperse phase are clusters of closely-packed droplets with some volumes of immobilized oil. The increase of shear rates at all upward flow curves is accompanied by a

corresponding decrease of apparent viscosity $\eta = \sigma/\dot{\gamma}$; hence, for all ϕ the emulsions may be classified as shear-thinning.

In modern rheological theories[13-15] the degree of structuring (state of flocculation) is usually characterized by a shear-dependent parameter λ which, in the first approximation, may be found from the interrelation of the measured viscosity η (current structure) and high-shear viscosity η_∞ (broken structure): $\eta = \eta_\infty(1 + \lambda^n)$.[13, 14] For qualitative analysis of the degree of initial structuring λ_{init}, we identified initial (low-shear) and high-shear conditions with shear rates of 0.1 s^{-1} and 437 s^{-1}, respectively and used n = 4. The obtained step-like dependence of $\lambda_{init} = \eta_{0.1}/\eta_{437} - 1$ on the emulsions water cut ϕ is shown at the left of Figure 3. The corresponding characteristic water cuts and emulsion morphologies A-F, suggested in ref.[7], are illustrated at the center of Figure 3. (A.) - At small water cuts, the studied emulsions evidently are dispersions of independent clusters of flocculated water droplets. (B.) – at $\phi \approx 0.15$, some clusters start to form chain-like aggregates, as evidenced by a minimum at $d\eta/d\phi$ derivatives. (C.) – Above $\phi \approx 0.18$ (percolation threshold for clusters), the clusters start to form extended loose networks ("fractal gels of clusters"). (D.) - At $\phi \approx 0.30$, primary clusters become "jammed" ("crowded"); at rest, they loose their freedom of thermally-activated movement as independent entities, and the resulting emulsion morphology is that of a loose emulsion-gel network of water droplets, spanning the sample ("fractal gels of droplets").[16] In more concentrated emulsions, "tight emulsion-gels" are formed as a result of "jamming" of individual water droplets.[17-19] The onset of these processes is characterized by two specific mechanisms: colloidal "glass transition" at $\phi \approx 0.58$ (E.); and "random close packing" at $\phi \approx 0.64$ (F). High packing values in tight emulsion-gels are achieved as a result of increased polydispersity of water droplets. Below $\phi \approx 0.74$ (hexagonal

close packing of monodisperse spheres) tight gels may be characterized as “soft” (plastic), while at higher ϕ “brittle” (fracturing) gels[18-21] are observed (G.). In these highly concentrated emulsions vorticity banding flow is the result of a “fracture type of mechanism which involves the coalescence of many emulsion droplets along a slip or fracture plain”.[20]

The above morphologies are developed already at the stage of emulsification, as revealed by analysis of droplet size distributions in samples from upper layers of as-prepared, non-sheared emulsions. The details of this analysis will be published elsewhere; the right part of Figure 3 illustrates the effect of water cut on the value of polydispersity index (the ratio of volume average diameter to number average diameter). Note the almost monodisperse character of fractal emulsion-gels (D.).

3.2 Hysteresis Loop Area as a Function of Water Cut

A sensitive measure of the degree of internal structuring in dispersed systems is an area of hysteresis loop at flow curves.[9] While the area S_{up} under the upward flow curve represents the mechanical energy input into the system, loop area S_{loop} is directly linked with the physical energy needed to overcome the resistance for breakdown and buildup of the internal structure. Figure 4 shows the effect of water cut in studied emulsions on the relative hysteresis loop area S_{loop}/S_{up}. These results clearly support the existence of earlier suggested multiple structures in petroleum W/O emulsions. Namely, a loop area is small in cluster emulsion morphologies (A.), (B.) at low ϕ, and sharply increases at the percolation threshold (C.) of $\phi \approx 0.18$. This increase terminates at “jamming” conditions for droplet clusters at $\phi \approx 0.30$ (D.) and the emerging fractal gels of droplets are characterized by nearly constant hysteresis loop areas. Another step-like rise of loop area (E.) is observed near conditions of “jamming” for water droplets at $\phi \approx 0.56$-0.58.

Formation of closely packed emulsion gels commences at $\phi \approx 0.64$ (F.) and is accompanied by a relatively slow increase of loop area, followed by a sharp decrease after the onset of vorticity banding in "brittle" gels with ϕ above ca. 0.77 (G.).

3.3 Time dependencies. Positive and Negative Thixotropic Behavior

Time dependencies of emulsion flow properties were studied in the Brookfield viscometer. At small water cuts, a conventional (positive) thixotropic behavior[9] was observed, as illustrated in Figure 5A. Namely, for each constant shear rate at upward flow curves, relative shear stress $\tau_{rel} = \tau(t)/\tau(0)$ decreased with time to a certain steady state value. Accordingly, at downward flow curves shear stress always increased with time. A qualitatively different time behavior was observed in samples with loose ("fractal") emulsion-gel initial morphologies, at water cuts $0.18 \leq \phi \leq 0.64$, as shown in Figure 5B for the upward flow curve. In this case, positive thixotropy (decrease of shear stress) was present only at high shear rates, while at low $\dot{\gamma}$, shear stresses increased with time – a behavior classified as negative thixotropy.[9]

For further analysis, the initial thixotropic behavior was quantitatively characterized by the increment of relative shear stress during 1 minute after the change of shear rate, $\Delta\tau_{rel}/\Delta t$. Accordingly, at upward flow curves, $\Delta\tau_{rel}/\Delta t < 0$ corresponds to positive thixotropy, while $\Delta\tau_{rel}/\Delta t > 0$ signifies negative thixotropy. Figure 6 illustrates the effects of shear rate on thixotropy, typical for emulsions with shear stress plateau (cf. Figure 2C). The upper part of the Figure 6 shows that at lowest shear rates a strong negative thixotropy is observed. With increasing $\dot{\gamma}$, the rate of negative thixotropy gradually decreases and becomes negligible at a certain critical shear rate $\dot{\gamma}^*$. Another critical value $\dot{\gamma}_C$ corresponds to an onset of a persistent

positive thixotropy. The lower part of Figure 6 shows that these critical shear rates coincide with the beginning and the end of stress plateau. Note, that the beginning of this plateau is the upper limit of a low-shear seemingly Newtonian behavior of these emulsions, without any apparent yield stress (cf. Figure 2B).

Previously,[7] the end of flow curve plateau was shown to be a signature of a specific process, break-up of an emulsion-gel structure, after which flow-induced evolution of emulsions with various water cuts may be described by a universal master curve. Hence, $\dot{\gamma}_C$ values may be regarded as material parameters of studied emulsions. The inset in Figure 6 shows that the corresponding gel-break stresses τ_C are closely related to the yield stresses τ_0 obtained from Herschel-Bulkley's fits to the flow curves at $\dot{\gamma} > \dot{\gamma}_C$:

$$\tau = \tau_0 + \eta_{HB}\dot{\gamma}^n \qquad (1)$$

where η_{HB} is a Herschel-Bulkley viscosity (consistency) and n is a power law exponent.

On the other hand, the second characteristic shear rate $\dot{\gamma}^*$ in Figure 6 appears to depend on details of the particular experimental procedure, as discussed below.

The canonical theories of yield stress fluids assume that the material is always homogeneous and is solid (does not flow) until a critical shear stress is exceeded. Above that stress the material yields and subsequently flows homogeneously. The Herschel-Bulkley model is widely used to describe such behavior. However, recent very precise experiments strongly suggest that the idealized Herschel-Bulkley behavior may be present only above a certain critical shear rate, $\dot{\gamma}_C$.[12-17,22-31] Below this shear rate, the flow observed in finite-time experiments is necessarily inhomogeneous in the direction normal to the flow. Most frequently, there appear a

layer sheared with $\dot{\gamma}_C$ close to the shearing wall and a non-sheared, solid-like layer.[23] The observed manifestations of these spatial inhomogeneities (shear banding,[30] shear localization,[23] lubricated flow,[32] wall slip,[23] local jamming[27]) should not be dismissed as artifacts,[24] as they are intrinsic properties of yield stress fluids that are always present at low enough shear rates. If in a finite-time experiment the globally imposed shear rate is increased to $\dot{\gamma}_C$, it is not the shear rate in the sheared region that increases, but rather the extent of the sheared region which grows - to fill the entire gap of the shear cell exactly at the critical shear rate. As a consequence of inhomogeneities, "obvious Newtonian flows" may be observed in yield stress samples even at shear rates as low as 10^{-5} - 10^{-7} s^{-1} at the limited time frames involved in the measurements.[22] At any constant shear rate below a critical value, the sample slowly evolves with time until a "solid" band eventually fills the rheometer's gap and a steady-state is attained, with the measured shear stress equal to τ_0.[22,23,25,28] The duration of the transient regime decreases as a power law with the applied shear rate and this power law behavior does not depend on the gap width and on the boundary conditions for a given sample.[28] Non-steady, heterogeneous flows could be observed for as long as a day at shear rates of 10^{-1} s^{-1},[25,28] and from weeks to months below 10^{-5} s^{-1}.[22] Hence, experiments of infinite duration are required to obtain a steady state flow curve at all shear rates employed[23] and the time-dependent behavior of the yielding process is directly responsible for the diverse flow curves obtained, due to the different time frames involved in the measurements. In particular, at any employed time frame, there should appear another characteristic shear rate $\dot{\gamma}^* < \dot{\gamma}_C$ above which the practically steady states with $\tau \approx \tau_0$ are observed. Hence, at the measured flow curves a stress plateau should appear at $\dot{\gamma}^* < \dot{\gamma} < \dot{\gamma}_C$, the beginning of which shifts to lower shear rates with increased duration of an experiment. Without

explicitly referring to the phenomena of shear banding, the above scenario was effectively accounted for in Papanastasiou's revision of the Herschel-Bulkley model[32,33] which may be written as:

$$\tau = \tau_0[1 - \exp(-m\dot{\gamma})] + \eta_{HB}\dot{\gamma}^n \qquad (2)$$

where *m* is a stress growth exponent, which has a dimension of time.

On the basis of these arguments, we interpret the value of $\dot{\gamma}^*$ in Figure 6 as the above discussed characteristic shear rate, closely associated with the Papanastasiou's parameter *m*. In support of this interpretation, Figure 7 shows flow curves plotted for different times (0.5 and 3 min) after each change of shear rate in Brookfield viscometer. The thick line is a Hershel Bulkley's fit to high-shear rate data, which is expected to provide a large-time steady state limit for $\dot{\gamma} < \dot{\gamma}_C$. The thin line fits to experimental data show that evolution of flow curves with increasing time is well accounted for by Papanastasiou's equation (2) with an increasing stress growth exponent *m*. Furthermore, Figure 7 confirms that the characteristic shear rate $\dot{\gamma}^*$ (above which a steady state apparently is attained) is not a material parameter, but a time-dependent one as it continuously moves to lower values with increasing *m*.

3.4 Flow Phase Diagrams

The above defined critical parameters $\dot{\gamma}_C$ and τ_C are upper boundaries for shear rate and shear stress intervals at which shear banding may arise and negative thixotropy may be observed. Another set of critical parameters includes water cuts ϕ, delimiting zero-shear emulsion morphologies A-F (cf. Figure 3). Combining these three data sets, it is possible to construct two non-equilibrium "flow phase diagrams",[34] presented in Figures 8 and 9.

Positive thixotropy in sheared samples is associated with gradual evolution of emulsion structure at the microscopic droplet level. The process involved are break-up of droplet clusters and aggregates of clusters in the homogeneous "flow phase", and droplet coalescence along fractures in vorticity banding "flow phase" V.B. On the other hand, negative thixotropy reflects evolution of the macroscopic flow structure and is basically dictated by the displacement of the interface between the sheared and unsheared regions.[29-31] As discussed above, it is associated with evolution from radial banding "flow phase" R.B. to solid-like plastic "flow phase" P.F (with a constant shear stress) in limited-time experiments. It should be noted, that the precise mechanisms of plastic behavior in emulsions still raise many questions[18-21] and apparently are not similar in different emulsion morphologies. E.g., at $\phi > 0.70$-0.74 the main processes most probably are those of fracturing and fracture elongation.[20] In emulsions with $0.58 < \phi < 0.7$, the stress relaxes instead by means of microscopically localized yield events, which do not seem to persist at preferred places, but occur throughout the material.[21,35]

Both τ - ϕ and $\dot{\gamma}$ - ϕ diagrams in Figures 8 and 9 show that for cluster morphologies with $\phi < 0.18$, the homogeneous "flow phase" is observed at any shear stresses or shear rates. For all gel morphologies with ϕ below ca. 0.8, homogeneous flow behavior is observed for shear stresses above τ_C, or shear rates above $\dot{\gamma}_C$. For highly concentrated tight gels with $\phi > 0.8$, the regions with $\tau > \tau_C$ ($\dot{\gamma} > \dot{\gamma}_C$) correspond to V.B. flow. At the τ-ϕ diagram of Figure 8, the conditions for plastic "flow phase" coincide with the critical boundary $\tau = \tau_C$ and for all tight droplet gels with $\phi>0.64$ no flow is observed with smaller shear stresses. For loose cluster-gel and droplet-gel morphologies, with $0.18 < \phi < 0.58$, flow with $\tau < \tau_C$ is possible in limited-time experiments via formation of the R.B "flow phase". At the $\dot{\gamma}$ - ϕ diagram of Figure 9, loose gels below the critical

boundary $\dot{\gamma} = \dot{\gamma}_C$ exhibit both R.B. flow with time dependent τ, and P.F. flow with $\tau = \tau_C$. The hatched regions at both flow phase diagrams correspond to emulsions with water cuts above "glass transition" at ϕ = 0.56-0.58 but below "maximum random jamming" at $\phi \approx 0.64$ (cf. discussion of Figure 2). On the basis of the obtained experimental data it is not yet possible to make any reliable conclusions on flow structure at these water cuts. Note also a peculiar feature of the $\dot{\gamma}$ - ϕ flow phase diagram in Figure 9. Namely, the experimental $\dot{\gamma}_C$ exhibit a tendency for diverging in the vicinity of the cluster percolation threshold at $\phi \approx 0.18$. The exact mechanisms of such behavior are not clear at the moment and require further investigations. A possible cause may be coexistence of the cluster and of the loose-gel morphologies at these water contents.

4. CONCLUSIONS

In this paper, factors affecting the apparent rheological behavior of native water in crude oil emulsions are examined experimentally in the Couette-type viscomeers. The studied emulsions were found to be shear-thinning and thixotropic fluids over shear stress and shear ranges of industrial interest for petroleum production, storage, and transport. The details of morphology (micro- and macrostructure) appear to be the main characteristics, from an internal point of view, that are responsible for the complex rheology of petroleum emulsions. Without insight into the structure of these fluids, an observed rheological behavior can be misinterpreted or attributed to experimental error or other extraneous factors. In particular, the parameters of "normal" positive thixotropy exhibit step-like changes in emulsions with increasing water cut as a result of development of multiple morphologies on the droplet level - "cluster fluid", "fractal gel of clusters", "fractal gel of droplets", "soft tight gel of droplets", "brittle tight gel of droplets". The underlying structure-breaking mechanisms of positive thixotropy also evolve from localized

randomly distributed microscopic events in emulsions with low and moderate water cuts to development of macroscopic extended fractures in “brittle tight gels”. In turn, “anomalous” negative thixotropy appears to be an inherent property of limited-time experiments and is governed by structure evolution of the entire macroscopic flow – from radial banding to homogeneous. The results reported here are expected to provide new insights into some problems related to the design and development of processes for recovery and transport of petroleum emulsions and to allow practitioners to discriminate real from transient/phantom phenomena present in their own measurements and in the literature. E.g., one of the immediate practical recommendations may be the following method for destabilization of concentrated emulsions in a production well. It is suggested that emulsions are treated by adding water/brine to increase volume fractions above 0.70 – 0.74. The produced fluids are expected to be “brittle gels”, exhibiting effective fracturing and droplet coalescence in flow through pumps and pressure gradients at pipeline valves.

REFERENCES

[1] Sjoblom, J., Aske, N., Auflem, I.H., Brandal, O., Havre, T.E., Saether, O., Westvik, A., Johnsen, E.E., and Kallevik, H. (2003) Our current understanding of water-in-crude oil emulsions. Recent characterisation techniques and high pressure performance. *Adv. Colloid Interface Sci.*, 100-102: 399-473.

[2] Sjoblom, J. (2006) *Emulsions and Emulsion Stability, 2d ed.*; CRC Press: New York.

[3] Aomari, N., Gaudu, R., Cabioch, F., and Omari, A. (1998) Rheology of water in crude oil emulsions. *Colloid Surface A*, 139 (1): 13 –20.

[4] Sullivan, A.P. and Kilpatrick, P.K. (2002) The Effects of Inorganic Solid Particles on Water and Crude Oil Emulsion Stability. *Ind. Eng. Chem. Res.*, 41 (14): 3389-3404.

[5] Urdahl, O. and Sjoblom, J. (1995) Water-in-crude oil emulsions from the Norwegian Continental Shelf. A stabilization and destabilization study. *J. Dispers. Sci. Technol.*, 16 (7): 557-574.

[6] Bridie, A.L., Wanders, Th.W., Zegveld, W., and van der Heijde, H.B. (1980) Formation. Prevention and Breaking of Sea-Water-in-Crude-Oil Emulsions: Chocolate Mousse. *Mar. Pollut. Bull.*, 11: 343–348.

[7] Evdokimov, I.N., Efimov, Y.O., Losev, A.P., and Novikov, M.A. (2008) Morphological Transformations of Native Petroleum Emulsions. I. Viscosity Studies. *Langmuir*, 24 (14): 7124-7131.

[8] Evdokimov, I.N., Eliseev, N.Yu., and Iktisanov, V.A. (2005) Excess density in oilfield water - crude oil dispersions. *J. Colloid Interface Sci.*, 285 (2): 795-803.

[9] Barnes, H.A. (1997) Thixotropy - a review. *J. Non-Newton. Fluid Mech.*, 70 (1-2): 1-33.

[10] Golemanov, K., Tcholakova, S., Kralchevsky, P.A., Ananthapadmanabhan, K.P., and Lips, A. (2006) Latex-Particle-Stabilized Emulsions of Anti-Bancroft Type. *Langmuir*, 22 (11), 4968-4977.

[11] Chen, Q., Yu, W., and Zhou, C. (2008) Transient stresses and morphology of immiscible polymer blends under varying shear flow. *Colloid Surface A*, 326 (3): 175–183.

[12] Dhont, J.K.G. and Briels, W.J. (2008) Gradient and vorticity banding. *Rheol. Acta*, 47(3), 257–281.

[13] Coussot, P., Nguyen, Q.D., Huynh, H.T., and Bonn, D. (2002) Avalanche behavior in yield stress fluids. *Phys. Rev. Lett.*, 88 (17): 175501.

[14] Ragouilliaux, A., Coussot, P., Palermo, T., and Herzhaft, B. (2009) Modeling Aging and Yielding of Complex Fluids: Application to an Industrial Material. *Oil Gas Sci. Technol.,* 64 (5): 571-581.

[15] Roussel, N. (2006) A thixotropy model for fresh fluid concretes: Theory, validation and applications. *Cement Concrete Res.*, 36 (10): 1797–1806.

[16] Bibette, J., Mason, T.G., Gang, H., Weitz, D.A., and Poulin, P. (1993) Structure of adhesive emulsions. *Langmuir*, 9 (12): 3352–3356.

[17] Mason, T.G., Graves, S.M., Wilking, J.N., and Lin, M.Y. (2006) Effective structure factor of osmotically deformed nanoemulsions. *J. Phys. Chem. B*, 110 (44), 22097–22102.

[18] Mason, T.G., Bibette, J., and Weitz, D.A. (1996) Yielding and Flow of Monodisperse Emulsions. *J. Colloid Interface Sci.*, 179 (2)**,** 439–448.

[19] Mason, T.G. (1999) New fundamental concepts in emulsion rheology *Curr. Opin. Colloid Interface Sci.*, 4 (3): 231-238

[20] van Aken, G.A. and Zoet, F.D. (2000) Coalescence in highly concentrated coarse emulsions. *Langmuir*, 16(18): 7131-7138.

[21] Benito, S., Bruneau, C.-H., Colin, T., Gay, C., and Molino, F. (2008) An elasto-visco-plastic model for immortal foams or emulsions. *Eur. Phys. J. E*, 25 (3): 225–251.

[22] Tiu, C., Guo, J., and Uhlherr, P.H.T. (2006) Yielding Behaviour of Viscoplastic Materials *J. Ind. Eng. Chem.*, 12 (5): 653-662.

[23] Møller, P.C.F., Mewis, J., and Bonn, D. (2006) Yield stress and thixotropy: on the difficulty of measuring yield stresses in practice. *Soft Matter*, 2: 274–283

[24] Ovarlez, G., Bertrand, F., and Rodts, S. (2006) Local determination of the constitutive law of a dense suspension of noncolloidal particles through magnetic resonance imaging. *J. Rheol.*, 50 (3): 259-292.

[25] Møller, P.C.F., Fall, A, and Bonn, D. (2009) Origin of apparent viscosity in yield stress fluids below yielding. *Europhys. Lett.*, 87 (3): 38004.

[26] Bécu, L., Manneville, S., and Colin, A. (2006) Yielding and flow in adhesive and non-adhesive concentrated emulsions. *Phys. Rev. Lett*., 96: 138302.

[27] Manneville, S. (2008) Recent experimental probes of shear banding. *Rheol. Acta*, 47(3): 301-318.

[28] Divoux, T., Tamarii, D., Barentin, C., and Manneville, S. (2010) Transient Shear Banding in a Simple Yield Stress Fluid. arXiv:1003.0161v1 [cond-mat.soft].

[29] Coussot, P., Tocquer, L., Lanos, C., and Ovarlez, G. (2009) Macroscopic vs. local rheology of yield stress fluids. *J. Non-Newt. Fluid Mech.*, 158 (1-3), 85-90.

[30] Ovarlez, G., Rodts, S., Château, X., and Coussot, P. (2009) Phenomenology and physical origin of shear localization and shear banding in complex fluids. *Rheol. Acta*, 48 (8): 831-844.

[31] Ragouilliaux, A., Coussot, P., Palermo, T., and Herzhaft, B. (2009) Modeling Aging and Yielding of Complex Fluids: Application to an Industrial Material. *Oil Gas Sci. Technol.,* 64 (5): 571-581.

[32] Papanastasiou, A.C., Macosko, C.W., and Scriven, L.E. (1986) Analysis of lubricated squeezing flow. *Int. J. Num. Meth. Fluids*, 6 (11): 819-839.

[33] Papanastasiou, T.C. (1987) Flow of Materials with Yield. *J. Rheol*., 31 (5): 385-404.

[34] Fielding, S.M. and Olmsted, P.D. (2003) Flow phase diagrams for concentration-coupled shear banding. *Eur. Phys. J. E Soft Matter*, 11 (1): 65-83.

(35) Witten, T.A. (1999) Insights from soft condensed matter. *Rev. Mod. Phys*., 71 (2): S367-S373.

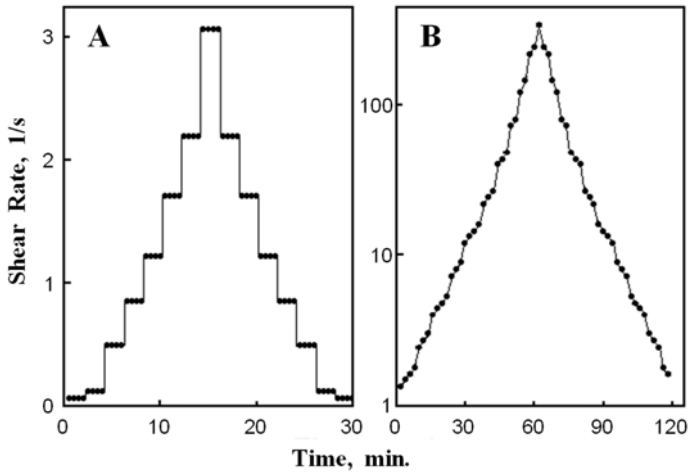

FIG. 1. Evolution of shear rates in thixotropic loop tests. A. - Brookfield viscometer; B. - Rheotest viscometer.

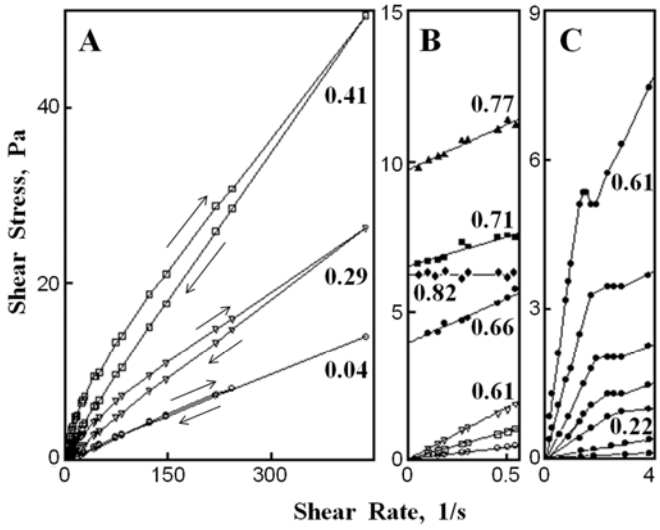

FIG. 2. A. - Typical loop test results for W/O emulsions with various water cuts ϕ , indicated in the figure. B. – Lowest-shear segments of the upward flow curves. C – Non-linear segments of upward flow curves for emulsions with ϕ>0.18-0.20.

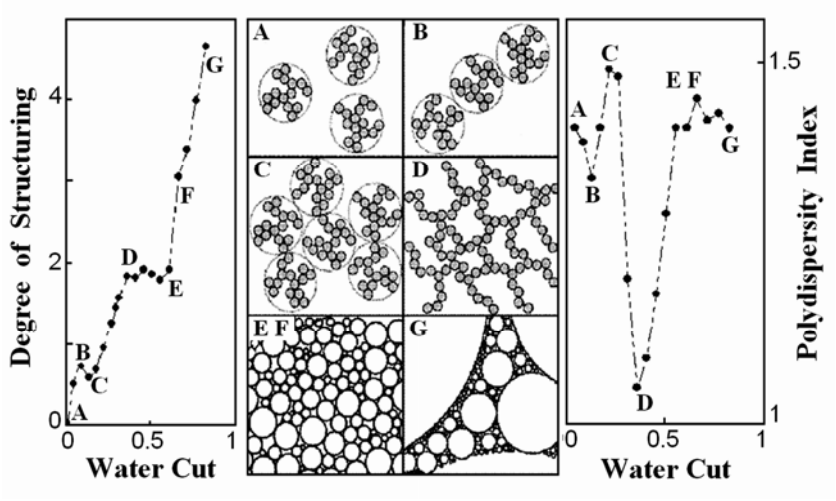

FIG. 3. Left – the degree of initial structuring in non-sheared emulsions as a function of water cut. Center – characteristic emulsion morphologies (after ref.[7]). Right – polydispersity of water droplets in non-sheared emulsions.

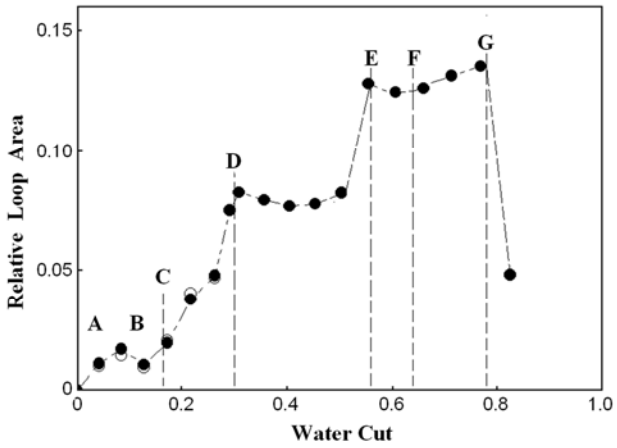

FIG. 4. Relative hysteresis loop area as a function of water cut in emulsions. Filled symbols – Rheotest viscometer, open symbols - Brookfield viscometer.

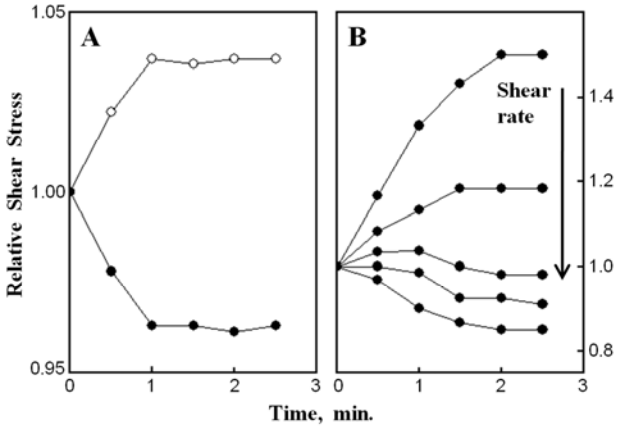

FIG. 5. Positive and negative thixotropy in petroleum emulsions. Filled symbols – upward flow curve; open symbols – downward flow curve. A - $\phi = 0.085$; $\gamma = 10\ s^{-1}$. B - $\phi=0.22$; $\gamma = 0.06$, 0.12, 0.49, 1.22 and 14.7 s^{-1}.

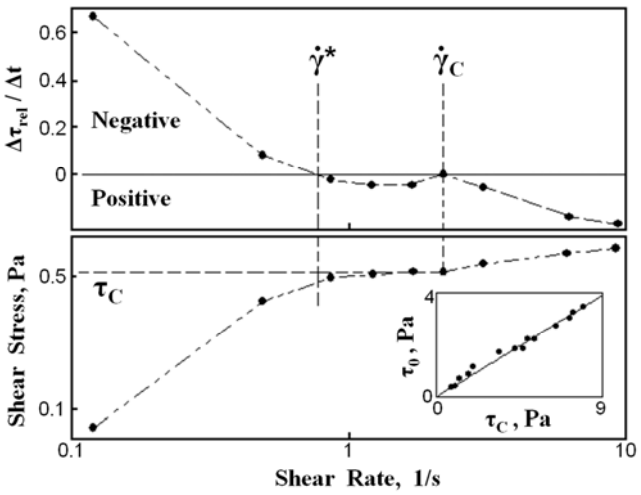

FIG. 6. Positive and negative thixotropy in emulsion with water cut ϕ=0.26. (Upward flow curve, Brookfield viscometer). Inset – relationship between the Herschel-Bulkley's yield stress τ_0 and the gel-break stress τ_C.

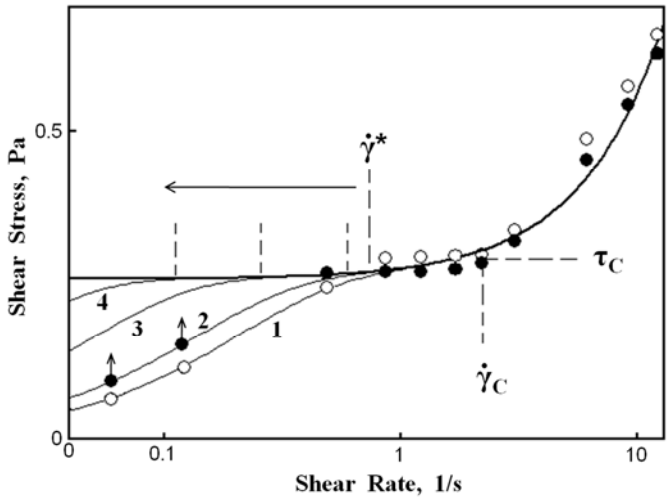

FIG. 7. Critical shear rates at upward flow curves (Brookfield viscometer, $\phi = 0.22$). Open and filled symbols denote the data for t = 0.5 and 3.0 min, respectively. Thick line – high-shear Herschel-Bulkley fit with $\tau_0 = 0.26$ Pa, $\eta_{HB} = 17.8$ mPa·s, n = 1.23. Thin lines 1-4 – Papanastasiou model with m = 4.9 s, 7.3 s, 20 s and 50 s, respectively.

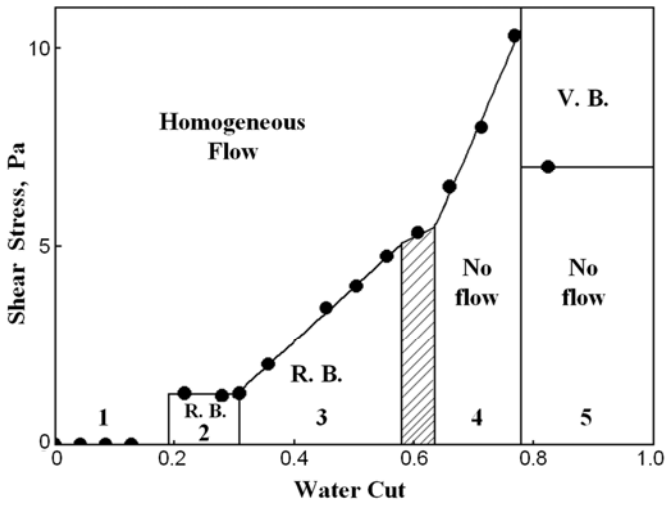

FIG. 8. Flow phase diagrams in terms of shear stress and water cut. Filled symbols – experimental τ_C values from upward flow curves. R.B. – radial banding flow; V.B. – vorticity banding flow. 1-4 – zero-shear emulsion morphologies defined in the text.

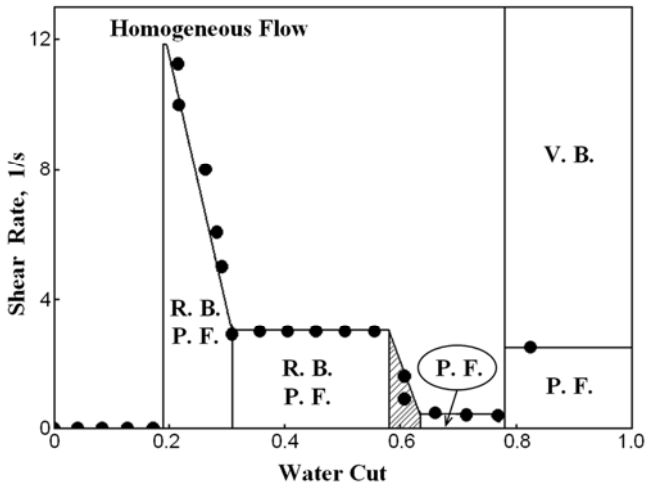

FIG. 9. Flow phase diagrams in terms of shear rate and water cut. Filled symbols – experimental $\dot{\gamma}_C$ values from upward flow curves. R.B. – radial banding flow; V.B. – vorticity banding flow; P.F. – solid-like plastic flow.